MASTER COPY: PLEASE KEEP THIS "MEMORANDUM OF TRANSMITTAL" BLANK FOR REPRODUCTION PURPOSES. WHEN REPORTS ARE GENERATED UNDER THE ARO SPONSORSHIP, FORWARD A COMPLETED COPY OF THIS FORM WITH EACH REPORT SHIPMENT TO THE ARO. THIS WILL ASSURE PROPER IDENTIFICATION. NOT TO BE USED FOR INTERIM PROGRESS REPORTS; SEE PAGE 2 FOR INTERIM PROGRESS REPORT INSTRUCTIONS.

MEMORANDUM OF TRANSMITTAL

U.S. Army Research Office
ATTN: AMSRL-RO-BI (TR)
P.O. Box 12211
Research Triangle Park, NC 27709-2211

- ☒ Reprint (Orig + 2 copies)
- ☐ Manuscript (1 copy)
- ☐ Technical Report (Orig + 2 copies)
- ☐ Final Progress Report (Orig + 2 copies)
- ☐ Related Materials, Abstracts, Theses (1 copy)

CONTRACT/GRANT NUMBER: **W911NF0410224 (46637-CI-MUR)**

REPORT TITLE:

Performance of Alamouti Space-Time Code in Time Varying Channels with Noisy Channel Estimates

Jittra Jootar, James R. Zeidler, John G. Proakis

In Proceedings of IEEE Wireless Communications and Networking Conference (WCNC)

pp. 498-503, New Orleans, Mar 2005

SUBMITTED FOR PUBLICATION TO (applicable only if report is manuscript):

Sincerely,

Dr. James Zeidler
Department of Electrical and Computer Engineering
University of California, San Diego

REPORT DOCUMENTATION PAGE

Form Approved
OMB NO. 0704-0188

Public Reporting burden for this collection of information is estimated to average 1 hour per response, including the time for reviewing instructions, searching existing data sources, gathering and maintaining the data needed, and completing and reviewing the collection of information. Send comment regarding this burden estimates or any other aspect of this collection of information, including suggestions for reducing this burden, to Washington Headquarters Services, Directorate for information Operations and Reports, 1215 Jefferson Davis Highway, Suite 1204, Arlington, VA 22202-4302, and to the Office of Management and Budget, Paperwork Reduction Project (0704-0188,) Washington, DC 20503.

1. AGENCY USE ONLY (Leave Blank)	2. REPORT DATE 16 March 2005	3. REPORT TYPE AND DATES COVERED Reprint: 01 June 2004 – 13 March 2005

4. TITLE AND SUBTITLE
Performance of Alamouti Space-Time Code in Time Varying Channels with Noisy Channel Estimates

5. FUNDING NUMBERS
W911NF0410224

6. AUTHOR(S)
Jittra Jootar, James R. Zeidler, and John G. Proakis

7. PERFORMING ORGANIZATION NAME(S) AND ADDRESS(ES)
University of California – San Diego
Department of Electrical and Computer Engineering
9500 Gilman Dr., La Jolla, CA 92093

8. PERFORMING ORGANIZATION REPORT NUMBER

9. SPONSORING / MONITORING AGENCY NAME(S) AND ADDRESS(ES)

U. S. Army Research Office
P.O. Box 12211
Research Triangle Park, NC 27709-2211

10. SPONSORING / MONITORING AGENCY REPORT NUMBER

11. SUPPLEMENTARY NOTES
The views, opinions and/or findings contained in this report are those of the author(s) and should not be construed as an official Department of the Army position, policy or decision, unless so designated by other documentation.

12 a. DISTRIBUTION / AVAILABILITY STATEMENT	12 b. DISTRIBUTION CODE
Approved for public release; distribution unlimited.	N/A

13. ABSTRACT (Maximum 200 words)
In this paper, we derive the theoretical performance of the Alamouti space-time code in time-varying Rayleigh fading channels with noisy channel estimates. The receiver algorithms presented in this paper are the maximum-likelihood (ML) symbol detector with the linear combining scheme, which was suggested by Alamouti \cite{Alamouti98}, and the ML space-time decoder. The bit error probability for the linear combining scheme and the sequence error probability for the ML space-time decoder are presented as functions of the pilot filter coefficients, the multi-path power profile, the normalized Doppler frequency, the pilot SNR and the data SNR. We also compare the bit error performance of the linear combining scheme with the bit error performance of the system without transmit diversity. The results indicate that the Alamouti space-time code with the linear combining scheme is outperformed by the no transmit diversity system at high Doppler frequency or low pilot SNR.

14. SUBJECT TERMS	15. NUMBER OF PAGES
N/A	6
	16. PRICE CODE N/A

17. SECURITY CLASSIFICATION OR REPORT	18. SECURITY CLASSIFICATION ON THIS PAGE	19. SECURITY CLASSIFICATION OF ABSTRACT	20. LIMITATION OF ABSTRACT
UNCLASSIFIED	**UNCLASSIFIED**	**UNCLASSIFIED**	**UL**

Enclosure 1

Performance of Alamouti Space-Time Code in Time-Varying Channels with Noisy Channel Estimates

Jittra Jootar, James R. Zeidler and John G. Proakis
Department of Electrical & Computer Engineering, University of California, San Diego, La Jolla, CA 92093-0407
Emails: jjootar@ucsd.edu, zeidler@ece.ucsd.edu, proakis@ece.ucsd.edu

Abstract— **In this paper, we derive the theoretical performance of the Alamouti space-time code in time-varying Rayleigh fading channels with noisy channel estimates. The receiver algorithms presented in this paper are the maximum-likelihood (ML) symbol detector with the linear combining scheme, which was suggested by Alamouti [1], and the ML space-time decoder. The bit error probability for the linear combining scheme and the sequence error probability for the ML space-time decoder are presented as functions of the pilot filter coefficients, the multi-path power profile, the normalized Doppler frequency, the pilot SNR and the data SNR. We also compare the bit error performance of the linear combining scheme with the bit error performance of the system without transmit diversity. The results indicate that the Alamouti space-time code with the linear combining scheme is outperformed by the no transmit diversity system at high Doppler frequency or low pilot SNR.**

I. Introduction

Over the last decade, space-time coding has gained attention both from the research community, as seen in a large number of space-time code related papers published, and the industrial community, where several space-time coding schemes are included as parts of future wireless communication standards. In this paper, we focus on the simple space-time code suggested by Alamouti [1], which was adopted as the space-time transmit diversity (STTD) mode in the 3^{rd} generation UMTS-WCDMA standard [2]. In [1], Alamouti also suggested a low complexity linear combining scheme which, under the assumptions of perfect channel state information (CSI) and quasi-static channels, can completely eliminate the interference from the other symbol in the codeword. As the result, this linear combiner can be used with the ML-symbol detector to achieve the same performance as the maximum-ratio combining (MRC) of the diversity branches, which is also equal to the performance of the more complicated ML space-time decoder [1], [3].

When the channels are not quasi-static, however, the interference is not completely eliminated by the linear combiner (with perfect CSI) causing a performance degradation [4], [5]. Under this condition, the ML symbol detector with an interference suppression scheme or the ML space-time decoder should be used to mitigate the effect from the time-varying fading channels [3], [4]. In addition to impairing the system performance through the interference, the time-varying fading also impairs the system through channel estimation error. When the channels fade rapidly at a high Doppler frequency, the channel estimates derived from the received pilot signals become more unreliable, thus degrading the performance of the coherent detection scheme. It has been shown that, when the noisy channel estimates are used, the linear combining scheme cannot correctly eliminate the signal contribution from the other symbol resulting in interference even in the quasi-static channels [5]–[10].

This research was supported by Core Grant No. 02-10109 sponsored by Ericsson.

Given the close relationship between the Doppler frequency and the channel estimation error and also their effects on the interference in the STTD system, it is desirable to evaluate the performance of the STTD system by taking into account these factors. Previous studies have focused on one of these factors in isolation, e.g., in [3] the authors derived the analytical performance of a zero-forcing linear detector and a decision-feedback detector assuming perfect CSI and rapid-fading channels. In addition, an analysis assuming imperfect CSI in quasi-static fading channels was presented in [6]–[9]. In this paper, the the objective is to generalize the existing analyses by providing the theoretical performance of the STTD system assuming imperfect CSI and rapid-fading channels. Two detection schemes are considered in this paper, namely, the *low complexity* ML symbol detector with the linear combining scheme and the *high complexity* ML space-time decoder.

This paper is organized as follows. Section II describes the system model. The performance analysis for the linear combining scheme and the ML space-time decoder are presented in section III. Discussions of the results and conclusions are presented in section IV and section V, respectively.

II. System model

The system under consideration is a downlink BPSK DS-CDMA system with two transmit antennas at the base station and one receive antenna at the mobile station. There are two pilot sequences, one from each transmit antenna, where each antenna uses a distinct orthogonal code. There are also two data sequences but, unlike the pilot sequences, both transmit antennas use the same orthogonal code for the data sequences. For simplicity, we also assume that the pilot channels and the

 0-7803-8966-2/05/$20.00 © 2005 IEEE

data channels have the same spreading gain, which results in the symbol period τ.

The channels are assumed to be time-varying Rayleigh fading channels, where the fading coefficients are assumed to be zero-mean circularly symmetric complex Gaussian random variables. With sufficient transmit antenna spacing, the fading from different transmit antennas are assumed to be uncorrelated. When the channels are frequency-selective fading, we assume that each resolvable path fades independently and the multi-path interference is negligible due to sufficiently large spreading gain and good correlation-properties of the scrambling codes.

III. Performance analysis

For the rest of this paper, the following notation will be used. The lowercase bold letter denotes a column vector and the uppercase bold letter denotes a matrix. The superscripts $*, T, H$ denote the complex conjugate, the matrix transpose and the matrix hermitian, respectively. The matrix determinant is denoted by $|.|$ while the square identity and the square zero matrices of size n are denoted by $\mathbf{I}_n, \mathbf{0}_n$, respectively.

Without loss of generality, we consider only a two-symbol period of the system. The transmitted sequence using the modified Alamouti space-time code or STTD as specified in the UMTS-WCDMA standard [2] is shown in table I. Note that, since we consider BPSK, the complex conjugate can be ignored.

Assuming that the transmit energy per data symbol is E_s and the transmit energy per pilot symbol is 1, (equivalent to $E_s/2$ and $1/2$ per antenna, respectively), the baseband representation of the received signals assuming that the channels are flat-fading can be expressed as

$$\mathbf{r}_s = \begin{bmatrix} r_{s,1} \\ r_{s,2}^* \end{bmatrix} = \sqrt{\frac{E_s}{2}} \begin{bmatrix} \alpha_1 & -\beta_1 \\ \beta_2^* & \alpha_2^* \end{bmatrix} \begin{bmatrix} s_1 \\ s_2^* \end{bmatrix} + \begin{bmatrix} n_{s,1} \\ n_{s,2}^* \end{bmatrix}$$
$$r_{p,i}^1 = \frac{1}{\sqrt{2}}\alpha_i + n_{p,i}^1 \rightarrow \mathbf{r}_{p,i}^1 = [r_{p,i-M}^1 \, .. \, r_{p,i}^1 \, .. \, r_{p,i+M}^1]^T \quad (1)$$
$$r_{p,i}^2 = \frac{1}{\sqrt{2}}\beta_i + n_{p,i}^2 \rightarrow \mathbf{r}_{p,i}^2 = [r_{p,i-M}^2 \, .. \, r_{p,i}^2 \, .. \, r_{p,i+M}^2]^T,$$

where the subscript i, p and s indicate the time index, the pilot channel and the data channel, respectively. The superscripts 1 and 2 indicate the parameters associated with the first antenna and the second antenna, respectively. The noise $n_{p,i}^1$, $n_{p,i}^2$ and $n_{s,i}$ are assumed to be zero-mean circularly symmetric complex white Gaussian noise with variance σ_p^2, σ_p^2 and σ_s^2, respectively. The fading coefficients α_i and β_i, corresponding to the links from the first transmit antenna and the second transmit antenna, respectively, are uncorrelated with identical autocorrelation $\sigma_c^2 R(m)$, where $R(0)$ is normalized to unity.

TABLE I
MODIFIED ALAMOUTI SPACE-TIME CODE

Symbol time	Antenna 1	Antenna2
1	s_1	$-s_2^*$
2	s_2	s_1^*

At the receiver, the channel estimation is performed by $(2M+1)$-tap FIR filters (one filter for each resolvable path). The channel estimates, which are the output of the pilot filters, can be expressed as

$$\hat{\alpha}_i = \mathbf{h}^H \mathbf{r}_{p,i}^1, \quad \hat{\beta}_i = \mathbf{h}^H \mathbf{r}_{p,i}^2, \quad (2)$$

where the vector $\mathbf{h}$ denotes the pilot filter coefficients $[h_M \, .. \, h_0 \, .. \, h_{-M}]^T$.

A. Linear combing scheme

The linear combining scheme suggested by Alamouti [1] can be written in the vector form

$$\begin{bmatrix} z_1 \\ z_2^* \end{bmatrix} = \begin{bmatrix} \hat{\alpha}_1^* & \hat{\beta}_2 \\ -\hat{\beta}_1^* & \hat{\alpha}_2 \end{bmatrix} \mathbf{r}_s = \sqrt{\frac{E_s}{2}}\, \mathbf{G} \begin{bmatrix} s_1 \\ s_2^* \end{bmatrix} + \begin{bmatrix} \tilde{n}_{s,1} \\ \tilde{n}_{s,2} \end{bmatrix}, \quad (3)$$

where $\tilde{n}_{s,1} = \hat{\alpha}_1^* n_{s,1} + \hat{\beta}_2 n_{s,2}^*$, $\tilde{n}_{s,2} = -\hat{\beta}_1^* n_{s,1} + \hat{\alpha}_2 n_{s,2}^*$ and

$$\mathbf{G} = \begin{bmatrix} \alpha_1\hat{\alpha}_1^* + \beta_2^*\hat{\beta}_2 & \alpha_2^*\hat{\beta}_2 - \beta_1\hat{\alpha}_1^* \\ \beta_2^*\hat{\alpha}_2 - \alpha_1\hat{\beta}_1^* & \beta_1\hat{\beta}_1^* + \alpha_2^*\hat{\alpha}_2 \end{bmatrix}. \quad (4)$$

Note that in the case of perfect CSI and quasi-static channels, where the linear combining scheme can eliminate the interference completely, $\mathbf{G}$ reduces to

$$\mathbf{G}_{\text{perfect}} = \begin{bmatrix} |\alpha_1|^2 + |\beta_1|^2 & 0 \\ 0 & |\alpha_1|^2 + |\beta_1|^2 \end{bmatrix} \quad (5)$$

with $\alpha_1 = \alpha_2$ and $\beta_1 = \beta_2$ [1].

Without loss of generality, we assume that $s_1 = s_2 = 1$. Also, since the bit error probability of the first symbol and the bit error probability of the second symbol are the same, we will consider only the first symbol. From (3), the output of the linear combiner corresponding to the first symbol is $z_1 = \hat{\alpha}_1^* r_{s,1} + \hat{\beta}_2 r_{s,2}^*$. The real part of z_1 can be written in the quadratic form $Re[z_1] = \mathbf{x}^H\mathbf{Q}\mathbf{x}$, where

$$\mathbf{x} = [r_{s,1} \;\; r_{s,2} \;\; \hat{\alpha}_1 \;\; \hat{\beta}_2]^T, \quad \mathbf{Q} = \frac{1}{2}\begin{bmatrix} \mathbf{0}_2 & \mathbf{I}_2 \\ \mathbf{I}_2 & \mathbf{0}_2 \end{bmatrix}. \quad (6)$$

Using the ML symbol detector, an error occurs when $Re[z_1]$ or $\mathbf{x}^H\mathbf{Q}\mathbf{x}$ is less than zero. The bit error probability P_b can then be expressed as

$$P_b = Pr\left[\mathbf{x}^H\mathbf{Q}\mathbf{x} < 0\right]. \quad (7)$$

Since $\mathbf{x}$ is a zero-mean correlated complex Gaussian random vector, the characteristic function of $\mathbf{x}^H\mathbf{Q}\mathbf{x}$ can be written as [11]

$$\Phi_{Re[z_1]}(s) = |\mathbf{I}_4 - 2s\mathbf{\Sigma}\mathbf{Q}|^{-1}, \quad (8)$$

where $\mathbf{\Sigma}$ denotes the covariance matrix of $\mathbf{x}$. From (1) and (2), the expression for the covariance matrix $\mathbf{\Sigma}$ can be found after some math

$$\mathbf{\Sigma} = \begin{bmatrix} \mathbf{A} & \mathbf{C} \\ \mathbf{C}^H & \mathbf{B} \end{bmatrix}, \quad (9)$$

where

$$\begin{aligned} \mathbf{A} &= E_s\sigma_c^2\left(1 + \bar{\gamma}_s^{-1}\right)\mathbf{I}_2, \\ \mathbf{B} &= \sigma_c^2\, \mathbf{h}^H\left(\frac{\mathbf{D}_0}{2} + \bar{\gamma}_p^{-1}\mathbf{I}_{2M+1}\right)\mathbf{h}\; \mathbf{I}_2, \\ \mathbf{C} &= \frac{\sqrt{E_s}\;\sigma_c^2}{2}\begin{bmatrix} \mathbf{w}_0^H\mathbf{h} & -\mathbf{w}_1^H\mathbf{h} \\ \mathbf{w}_{-1}^H\mathbf{h} & \mathbf{w}_0^H\mathbf{h} \end{bmatrix}, \end{aligned} \quad (10)$$

$\bar{\gamma}_p = \sigma_c^2/\sigma_p^2$ denotes the average pilot SNR or pilot E_p/N_o and $\bar{\gamma}_s = E_s\sigma_c^2/\sigma_s^2$ denotes the average data SNR or data E_b/N_o. $\mathbf{D}_e$ denotes a square matrix of size $2M+1$ with $\mathbf{D}_e(i,j) = R((e+i-j)\tau)$ and $\mathbf{w}_e$ is the $(M+1)^{th}$ column of $\mathbf{D}_e$.

Knowing $\mathbf{\Sigma}$, P_b can be evaluated by using the eigenvalues of $2\mathbf{\Sigma Q}$ ($\lambda_i, i = 1, ..., 4$) [12] and the residue theorem described as follows.

$$P_b = -\frac{1}{2\pi j}\int_{-\infty+j\epsilon}^{\infty+j\epsilon} \frac{1}{v\prod_{i=1}^{4}(1-jv\lambda_i)}dv \quad (11)$$

$$= -\text{Res}[\Phi_z(s)/s \text{ at LHP poles}], \quad (12)$$

where Res$[f(s)$ at $a]$ denotes the residue of $f(s)$ at $s = a$. The residue can be calculated by

$$\text{Res}\big[f(s) \text{ at } a\big] = \lim_{s\to a}\frac{p^{(n-1)}(s)}{(n-1)!}, \quad (13)$$

where $p(s) = (s-a)^n f(s)$ and $p^n(s)$ denotes the n^{th} derivative of $p(s)$. Alternatively, P_b can be found numerically by the Gauss-Chebyshev approximation [13]

$$P_b \approx \frac{1}{2n}\sum_{k=1}^{n}\left(Re[\Phi_z(c+jc\tau_k)] + \tau_k Im[\Phi_z(c+jc\tau_k)]\right), \quad (14)$$

where $\tau_k = \tan((2k-1)\pi/2n)$ and, in general, n between 32 and 64 is sufficient [13].

Although our analysis allows any values of $\mathbf{h}$, for simplicity, the $(2M+1)$-tap Wiener filter will be used throughout as an example in this paper. Using the Wiener filter as the pilot filter, the filter coefficients become

$$\mathbf{h} = \frac{1}{\sqrt{2}}\left(\frac{\mathbf{D}_0}{2} + \bar{\gamma}_p^{-1}\mathbf{I}_{2M+1}\right)^{-1}\mathbf{w}_0. \quad (15)$$

Substituting $\mathbf{h}$ from (15) into (10), we get

$$\mathbf{\Sigma} = \sigma_c^2\begin{bmatrix} E_s\left(1+\bar{\gamma}_s^{-1}\right)\mathbf{I}_2 & \sqrt{\frac{E_s}{8}}\begin{bmatrix}\varepsilon_0 & -\varepsilon_1\\ \varepsilon_1 & \varepsilon_0\end{bmatrix} \\ \sqrt{\frac{E_s}{8}}\begin{bmatrix}\varepsilon_0 & \varepsilon_1\\ -\varepsilon_1 & \varepsilon_0\end{bmatrix} & \frac{\varepsilon_0}{2}\mathbf{I}_2\end{bmatrix}, \quad (16)$$

where

$$\begin{aligned}\varepsilon_0 &= \mathbf{w}_0^H\left(\mathbf{D}_0/2 + \bar{\gamma}_p^{-1}\mathbf{I}_{2M+1}\right)^{-1}\mathbf{w}_0\\ \varepsilon_1 &= \mathbf{w}_1^H\left(\mathbf{D}_0/2 + \bar{\gamma}_p^{-1}\mathbf{I}_{2M+1}\right)^{-1}\mathbf{w}_0.\end{aligned} \quad (17)$$

After some math, the eigenvalues of $2\mathbf{\Sigma Q}$ are found to be $\lambda_1 = \sigma_c^2\varepsilon_0(1+\Upsilon^{-1})$ and $\lambda_2 = \sigma_c^2\varepsilon_0(1-\Upsilon^{-1})$, both with the multiplicity of 2 with

$$\Upsilon = \left(\frac{4(1+\bar{\gamma}_s^{-1})}{\varepsilon_0} - \left(\frac{\varepsilon_1}{\varepsilon_0}\right)^2\right)^{-1/2}. \quad (18)$$

From (17) and (18), it can be proven that the poles of the characteristic function are $1/\lambda_1$ and $1/\lambda_2$ with $1/\lambda_2$ in the LHP and $1/\lambda_1$ in the RHP. P_b is then equal to minus the residue of $\Phi(s)/s$ at $1/\lambda_2$. Using the fact that the residue is invariant to the scaling of the poles (see appendix for proof), the compact form of the bit error probability can be calculated as follows

$$P_b = \lim_{s\to\frac{\sigma_c^2\varepsilon_0}{\lambda_2}}\frac{d}{ds}\left(\frac{\left(s-\frac{\sigma_c^2\varepsilon_0}{\lambda_2}\right)^2}{s\left(1-\frac{s\lambda_1}{\sigma_c^2\varepsilon_0}\right)^2\left(1-\frac{s\lambda_2}{\sigma_c^2\varepsilon_0}\right)^2}\right). \quad (19)$$

$$= \frac{1}{4}\left(2+\Upsilon\right)\left(1-\Upsilon\right)^2$$

For a sanity check, we compare our result in (19) with the perfect CSI result in the existing papers by setting $\bar{\gamma}_p \to \infty$. This results in $\varepsilon_0 = 2, \varepsilon_1 = 2R(\tau) = 2R(-\tau)$ and

$$\Upsilon = \left(2 + 2/\bar{\gamma}_s - R^2(\tau)\right)^{-1/2}. \quad (20)$$

In the limit when $R(\tau) = 0$ (very fast fading) or 1 (static channel) with perfect CSI, (19) and (20) reduce to

$$R(\tau) = 1 \to P_b = \frac{1}{4}\left(2+\sqrt{\frac{\bar{\gamma}_s}{\bar{\gamma}_s+2}}\right)\left(1-\sqrt{\frac{\bar{\gamma}_s}{\bar{\gamma}_s+2}}\right)^2 \quad (21)$$

$$R(\tau) = 0 \to P_b = \frac{1}{4}\left(2+\sqrt{\frac{\bar{\gamma}_s}{2\bar{\gamma}_s+2}}\right)\left(1-\sqrt{\frac{\bar{\gamma}_s}{2\bar{\gamma}_s+2}}\right)^2 \quad (22)$$

Note that (21) agrees with the result derived in [3], [9].

Although the bit error probability of s_1 and s_2 are equal, they are not independent. The approach suggested here does not lead to the exact sequence error probability of $[s_1\ s_2]$. Nevertheless, the upper bound of the error probability of the code sequence $[s_1\ s_2]$, P_2 can be found by the union bound of the bit error probability of s_1 and s_2, i.e.,

$$P_2 \le 2P_b. \quad (23)$$

B. ML space-time decoder

The ML space-time decoder is the optimal decoder. It chooses the codeword, which is the most likely to be transmitted given the received signals. Without loss of generality, we assume that the transmitted sequence is $[s_1\ s_2] = [1\ 1]$. Let $P_{[\hat{s}_1\ \hat{s}_2]}$ be the probability that the ML space-time decoder picks $[\hat{s}_1\ \hat{s}_2]$ given the transmitted sequence $[1\ 1]$. The union bound of the sequence error, which is the summation of all possible error patterns, can be written as

$$P_2 \le P_{[1\ -1]} + P_{[-1\ 1]} + P_{[-1\ -1]}. \quad (24)$$

Let $\tilde{P}_1 = P_{[1\ -1]}, \tilde{P}_2 = P_{[-1\ 1]}$ and $\tilde{P}_3 = P_{[-1\ -1]}$. The probabilities $\tilde{P}_i$ can be simplified to:

$$\tilde{P}_i = Pr\left(Re\left[z^i\right] < 0\right), \quad (25)$$

where

$$z^1 = -\sqrt{\frac{E_s}{2}}\left(r_{s,1}\hat{\beta}_1^* - r_{s,2}\hat{\alpha}_2^*\right) + \frac{E_s}{2}\left(\hat{\alpha}_1\hat{\beta}_1^* - \hat{\alpha}_2\hat{\beta}_2^*\right)$$

$$z^2 = \sqrt{\frac{E_s}{2}}\left(r_{s,1}\hat{\alpha}_1^* + r_{s,2}\hat{\beta}_2^*\right) + \frac{E_s}{2}\left(\hat{\alpha}_1\hat{\beta}_1^* - \hat{\alpha}_2\hat{\beta}_2^*\right)$$

$$z^3 = \sqrt{\frac{E_s}{2}}\ r_{s,1}(\hat{\alpha}_1 - \hat{\beta}_1)^* + \sqrt{\frac{E_s}{2}}\ r_{s,2}(\hat{\alpha}_2 + \hat{\beta}_2)^*$$

 0-7803-8966-2/05/$20.00 © 2005 IEEE

Using the same approach used in subsection III-A, we let $\mathbf{x}_{ML} = [r_{s,1}\ r_{s,2}\ \sqrt{\frac{E_s}{2}}\ \hat{\alpha}_1\ \sqrt{\frac{E_s}{2}}\ \hat{\alpha}_2\ \sqrt{\frac{E_s}{2}}\ \hat{\beta}_1\ \sqrt{\frac{E_s}{2}}\ \hat{\beta}_2]^T$. The metric $Re[z^i]$ corresponding to each error pattern can then be written in the quadratic form $Re[z^i] = \mathbf{x}_{ML}^H \mathbf{Q}_i \mathbf{x}_{ML}$, where

$$\mathbf{Q}_1 = \frac{1}{2}\begin{bmatrix} 0 & 0 & 0 & 0 & -1 & 0 \\ 0 & 0 & 0 & 1 & 0 & 0 \\ 0 & 0 & 0 & 0 & 1 & 0 \\ 0 & 1 & 0 & 0 & 0 & -1 \\ -1 & 0 & 1 & 0 & 0 & 0 \\ 0 & 0 & 0 & -1 & 0 & 0 \end{bmatrix} \tag{26}$$

$$\mathbf{Q}_2 = \frac{1}{2}\begin{bmatrix} 0 & 0 & 1 & 0 & 0 & 0 \\ 0 & 0 & 0 & 0 & 0 & 1 \\ 1 & 0 & 0 & 0 & 1 & 0 \\ 0 & 0 & 0 & 0 & 0 & -1 \\ 0 & 0 & 1 & 0 & 0 & 0 \\ 0 & 1 & 0 & -1 & 0 & 0 \end{bmatrix} \tag{27}$$

$$\mathbf{Q}_3 = \frac{1}{2}\begin{bmatrix} 0 & 0 & 1 & 0 & -1 & 0 \\ 0 & 0 & 0 & 1 & 0 & 1 \\ 1 & 0 & 0 & 0 & 0 & 0 \\ 0 & 1 & 0 & 0 & 0 & 0 \\ -1 & 0 & 0 & 0 & 0 & 0 \\ 0 & 1 & 0 & 0 & 0 & 0 \end{bmatrix} \tag{28}$$

The covariance matrix of $\mathbf{x}_{ML}$ can be shown to reduce to

$$\mathbf{\Sigma}_{ML} = \begin{bmatrix} \mathbf{A}_{ML} & \mathbf{C}_{ML} & \mathbf{D}_{ML} \\ \mathbf{C}_{ML}^H & \mathbf{B}_{ML} & \mathbf{0}_2 \\ \mathbf{D}_{ML}^H & \mathbf{0}_2 & \mathbf{B}_{ML} \end{bmatrix}, \tag{29}$$

where

$$\begin{aligned}
\mathbf{A}_{ML} &= E_s\sigma_c^2(1+\bar{\gamma}_s^{-1})\ \mathbf{I}_2 \\
\mathbf{B}_{ML} &= \frac{E_s\sigma_c^2}{2}\begin{bmatrix} \mathbf{h}^H\left(\frac{\mathbf{D}_0}{2}+\bar{\gamma}_p^{-1}\boldsymbol{\delta}_0\right)\mathbf{h} & \mathbf{h}^H\left(\frac{\mathbf{D}_{-1}}{2}+\bar{\gamma}_p^{-1}\boldsymbol{\delta}_{-1}\right)\mathbf{h} \\ \mathbf{h}^H\left(\frac{\mathbf{D}_1}{2}+\bar{\gamma}_p^{-1}\boldsymbol{\delta}_1\right)\mathbf{h} & \mathbf{h}^H\left(\frac{\mathbf{D}_0}{2}+\bar{\gamma}_p^{-1}\boldsymbol{\delta}_0\right)\mathbf{h} \end{bmatrix} \\
\mathbf{C}_{ML} &= \frac{E_s\sigma_c^2}{2\sqrt{2}}\begin{bmatrix} \mathbf{w}_0^H\mathbf{h} & \mathbf{w}_1^H\mathbf{h} \\ \mathbf{w}_{-1}^H\mathbf{h} & \mathbf{w}_0^H\mathbf{h} \end{bmatrix} \\
\mathbf{D}_{ML} &= \frac{E_s\sigma_c^2}{2\sqrt{2}}\begin{bmatrix} -\mathbf{w}_0^H\mathbf{h} & -\mathbf{w}_1^H\mathbf{h} \\ \mathbf{w}_{-1}^H\mathbf{h} & \mathbf{w}_0^H\mathbf{h} \end{bmatrix}
\end{aligned} \tag{30}$$

and $\boldsymbol{\delta}_e$ is a square matrix of size $2M+1$ with ones on the e^{th} diagonal (command $diag([1\ \ldots\ 1], e)$ in matlab), $\mathbf{w}_e$ and $\mathbf{D}_e$ are the same as defined before.

Equipped with $\mathbf{Q}_i$ and $\mathbf{\Sigma}_{ML}$, $\tilde{P}_i$ can be calculated using the residue theorem or the Gauss-Chebyshev approximation approach similar to the ones described in subsection III-A.

C. Multi-path

Assuming that all paths fade independently and there is no multi-path interference, the extension from the single-path to the multi-path is straight forward. The characteristic function of $Re[z]$ (or $Re[z^i]$) of the multi-path channels is basically the product of the characteristic functions of all paths. The error probability can be found using the residue theorem or the Gauss-Chebyshev approximation suggested before. Also, in order to make a fair comparison, the fading variance should

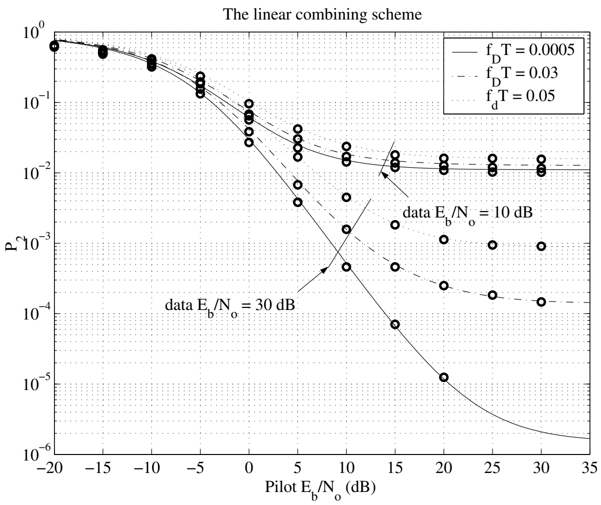

Fig. 1. The effect of speed, pilot E_p/N_0 and data E_b/N_0 on P_2

be normalized such that the sum of the fading variance in the multi-path case is equal to the fading variance in the flat-fading case, i.e., $\sum_{l=1}^{L} \sigma_{c,l}^2 = \sigma_c^2$, where $\sigma_{c,l}^2$ is the fading variance of the l^{th} path, and σ_c^2 is the fading variance in the flat-fading case.

IV. Results

In this section, we present numerical examples to illustrate the effect of the Doppler spread and the channel estimation error on the performance of STTD. Throughout this section, we assume that the fading autocorrelation function is the zeroth-order Bessel function of the first kind $J_0(2\pi f_D \tau)$, which is derived from Jakes' PSD [14], with f_D being the Doppler frequency. The pilot filter is assumed to be the Wiener filter optimized corresponding to the pilot E_p/N_o and the fading correlation.

Fig. 1 and 2 show the performance bounds of the linear combining scheme as shown in (23) and the ML space-time decoder as shown in (24), respectively, with the circles representing the simulation results. Comparing the simulation results and the analytical bounds, the bounds are shown to be reasonably tight especially at low P_2. Comparing fig. 1 and 2, we can see that the ML space-time decoder performs better than the linear combining scheme, especially at high Doppler frequency, high pilot E_p/N_o and high data E_b/N_o.

The effect of the channel estimation error on the system with no transmit diversity (noTD) is well known [15]. With the notations used in this paper, the bit error probability of noTD can be written as [15]

$$P_b = \frac{1}{2}\left(1 - \sqrt{\frac{\mathbf{w}_0^H\left(\mathbf{D}_0 + \bar{\gamma}_p^{-1}\mathbf{I}_d\right)^{-1}\mathbf{w}_0}{1+\bar{\gamma}_s^{-1}}}\right). \tag{31}$$

The bit error probability comparison between noTD and STTD (with the linear combining scheme) assuming that the data E_b/N_o is 30 dB is shown in fig. 3, where the z-axis shows

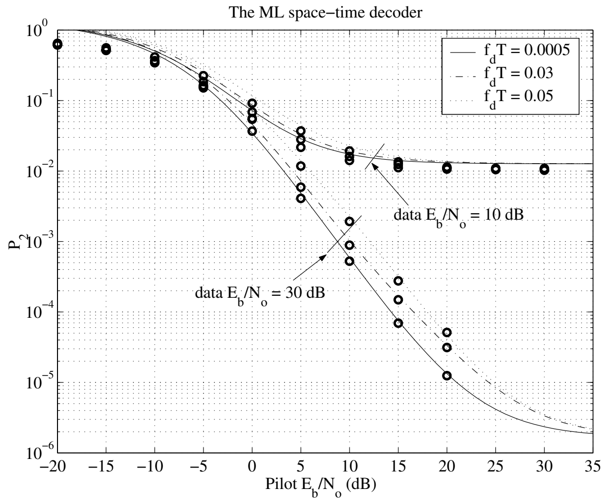

Fig. 2. The effect of speed, pilot E_p/N_0 and data E_b/N_0 on P_2

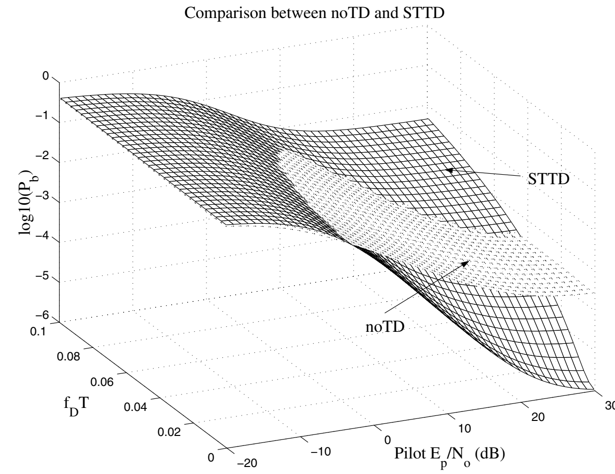

Fig. 3. Comparison between noTD and STTD

$\log_{10}(P_b)$. As expected, STTD with the linear combining scheme performs well when the channels do not change too rapidly and when the pilot E_p/N_o is high (accurate CSI). However, when the channels change rapidly or when the pilot E_p/N_o is small, STTD with the linear combining scheme is outperformed by noTD.

Fig. 4 shows the STTD performance in the frequency-selective fading channels, assuming that the two resolvable paths have the same average energy. Although the system still suffers from the Doppler spread, the performance gain from the path diversity is evidenced as seen in better performance floors at high pilot E_p/N_o, which are significantly lower than the performance floors corresponding to the flat-fading channels in fig. 1.

Although we have shown that the linear combining scheme is greatly affected by the channel estimation error and the Doppler frequency, we would like to point out that the choice of STTD decoding algorithm should depend on the operating condition of the respective system. For example, the bit error performance of the STTD system with the linear combining scheme corresponding to the UMTS-WCDMA 12.2 kbps downlink reference measurement channel assuming that the spreading factor is 128 (or $\tau^{-1} = 30$ KHz) is shown in fig. 5. In this figure, the bit error probability corresponding to the mobile speed of 3 kmph and 120 kmph for perfect CSI and noisy CSI (pilot E_p/N_o = 10 dB, Wiener filter with $M = 5$) are compared. Fig. 5 clearly shows that, if the desired bit error probability of the system is greater than 10^{-4}, the degradation from using the linear combining scheme is very small.

V. Conclusions

In this paper, we have derived the bit error probability for the linear combining scheme and the sequence error probability for the ML space-time decoder assuming that the Alamouti space-time scheme is used in a time-varying fading channel with noisy CSI. We have shown that the performance

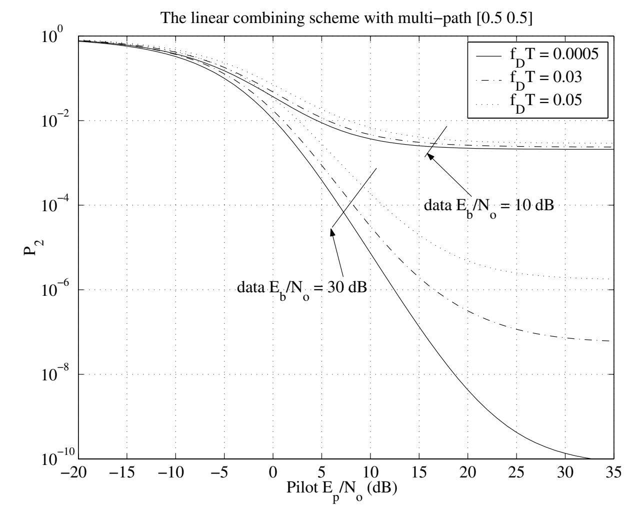

Fig. 4. The linear combining scheme in the multi-path fading channels

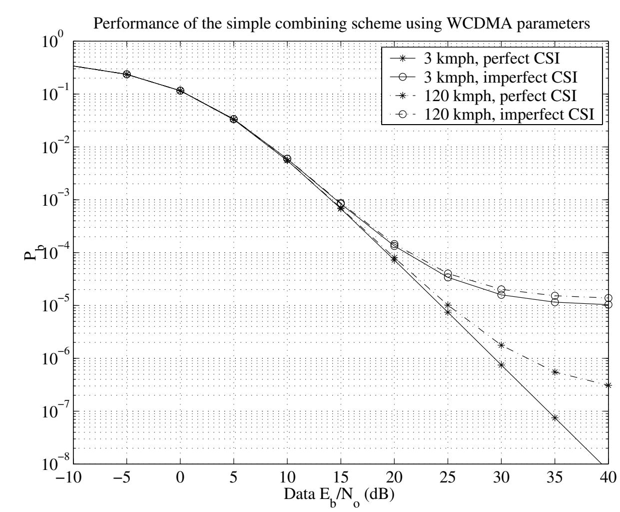

Fig. 5. Performance of the linear combining scheme using WCDMA parameters

 0-7803-8966-2/05/$20.00 © 2005 IEEE

of the linear combining scheme is degraded when the Doppler spread is increased, and the ML space-time decoder, which is more complex, is more tolerant to the Doppler spread as evidenced in smaller performance loss when the Doppler frequency is increased.

We have also shown that, although broadly accepted as a way to improve the system performance in fading channels, STTD does not always outperform the system without transmit diversity when the linear combining scheme is used. Thus, the deployment of STTD and the choice of the decoding scheme should be done with this constraint in mind. An example of the system, where the linear combining scheme with noisy channel estimates can be used in time-varying Rayleigh fading channels without noticeable performance degradation, is the 12.2 kpbs downlink reference channel described in the UMTS-WCDMA standard.

Although only simple cases were presented, we would like to note that the framework provided in this paper can be used with a wide range of assumptions. For example, an extension of the bit error analysis from BPSK to QPSK for the linear combining scheme can be done similarly to the extension presented in [15]. However one should keep in mind that, due to the crosstalk between the real part and the imaginary part, the bit error probabilities of I/Q bits are not independent. The extension of this analysis cannot provide the exact symbol error probability for the QPSK system but only the upper bound, which is the summation of the bit error probabilities of the I and Q bits. Also, because the noise variance corresponding to each resolvable path in the multi-path analysis need not be equal, we can also extend the analysis to find the performance when the multi-path interference, which is assumed to be equivalent to additional AWGN noise, is considered by setting the noise variance in each path to be the summation of the variance from the AWGN and the variance from the multi-path interference corresponding to that path.

APPENDIX
RESIDUES OF SCALED POLES

In this section, we show the proof that residues are invariant to the scaling of the poles. Consider the function $\Phi_z(s)/s$:

$$\begin{aligned}\frac{\Phi_z(s)}{s} &= \frac{1}{s\prod_{k=1}^{2d}(\lambda_i s-1)} = \frac{1}{s\prod_{k=1}^{2d}\lambda_i(s-1/\lambda_i)} \\ &= \frac{k_1}{s}+\frac{k_2}{s-1/\lambda_1}+\frac{k_3}{s-1/\lambda_2}+\frac{k_4}{(s-1/\lambda_2)^2} \\ &+\ldots+\frac{k_{n+2}}{(s-1/\lambda_2)^n}+\frac{k_{n+3}}{s-1/\lambda_3}+\ldots\end{aligned} \quad (32)$$

For generality, we assume that the multiplicity of $1/\lambda_2$ is n where $n > 1$.

Let $s = ay$, we get

$$\begin{aligned}\frac{\Phi_z(ay)}{ay} &= \frac{1}{ay\prod_{k=1}^{2d}(\lambda_i ay-1)} = \frac{1}{ay\prod_{k=1}^{2d}\lambda_i(ay-1/\lambda_i)} \\ &= \frac{k_1/a}{y}+\frac{k_2/a}{y-1/\lambda_1 a}+\frac{k_3/a}{y-1/\lambda_2 a}+\frac{k_4/a^2}{(y-1/\lambda_2 a)^2} \\ &+\ldots+\frac{k_{n+2}/a^n}{(y-1/\lambda_2 a)^n}+\frac{k_{n+3}/a}{y-1/\lambda_3 a}+\ldots\end{aligned}$$

Thus,

$$\begin{aligned}\frac{1}{y\prod_{k=1}^{2d}(ya\lambda_i-1)} &= \frac{k_1}{y}+\frac{k_2}{y-1/\lambda_1 a}+\frac{k_3}{y-1/\lambda_2 a} \\ &+\frac{k_4/a}{(y-1/\lambda_2 a)^2}+\ldots+\frac{k_{n+3}}{y-1/\lambda_3 a}+\ldots\end{aligned} \quad (33)$$

From (33), we can see that, when all λ_i are scaled to $a\lambda_i$, coefficients associated with the terms $(y-1/\lambda_i a)^{-1}$ are the same as the coefficients associated with $(y-1/\lambda_i)^{-1}$ in (32). This proves that the residue is invariant to the scaling of the poles.

REFERENCES

[1] S. M. Alamouti, "A simple transmit diversity technique for wireless communications," *IEEE J. Select. Areas Commun.*, vol. 16, pp. 1451–1458, Oct. 1998.
[2] 3GPP, "Technical specification group radio access network, physical channels and mapping of transport channels onto physical channels, 25.211."
[3] A. Vielmon, Y. Li, and J. R. Barry, "Performance of transmit diversity over time-varying Rayleigh-fading channels," in *Proc. IEEE Globecom 2001*, pp. 3242 – 3246, Nov. 2001.
[4] Y. Zhang and D. Li, "Performance of space-time transmit diversity over time-selective fading channels," in *Proc.* 9^{th} *IEEE Asia Pacific Conference on Communications (APCC)*, pp. 402–405, 2003.
[5] P. Schulz-Rittich, J. Baltersee, and G. Fock, "Channel estimation for DS-CDMA with transmit diversity over frequency selective fading channels," in *Proc. IEEE VTC Spring 2001*, pp. 1973 – 1977, May 2001.
[6] M. Stege, M. Bronzel, and G. Fettweis, "On the performance of space-time blockcodes," in *Proc. IEEE VTC Spring 2001*, pp. 2282–2286, May 2001.
[7] R. M. Buehrer and N. A. Kumar, "The impact of channel estimation error on space-time block codes," in *Proc. IEEE VTC Fall 2002*, pp. 1921–1925, Sept. 2002.
[8] H. Cheon and D. Hong, "Performance analysis of space-time block codes in time-varying Rayleigh fading channels," in *Proc. IEEE ICASSP'02*, pp. 2357 – 2360, May 2002.
[9] D. Gu and C. Leung, "Performance analysis of transmit diversity scheme with imperfect channel estimation," *Electronic Letters*, vol. 39, pp. 402–403, Feb. 2003.
[10] W. C. Ang and C. S. Ng, "Analysis of a transmit diversity scheme in fading channels and imperfect channel estimation," in *Proc. International Conference on Communication Systems 2002. (ICCS 2002)*, pp. 188–192, Nov. 2002.
[11] G. L. Turin, "The characteristic function of hermitian quadratic forms in complex normal variables," *Biometrika*, vol. 47, pp. 199–201, June 1960.
[12] J. G. Proakis, *Digital Communications*. New York: McGraw-Hill.
[13] E. Biglieri, G. Caire, G. Taricco, and J. Ventura-Traveset, "Simple method for evaluating error probabilities," *Electronic Letters*, vol. 32, pp. 191–192, Feb. 1996.
[14] W. C. Jakes, *Microwave Mobile Communications*. New Jersey: IEEE Press, 1994.
[15] J. K. Cavers, "An analysis of pilot symbol assisted modulation for Rayleigh fading channels," *IEEE Trans. Veh. Technol.*, vol. 40, pp. 686–693, Nov. 1991.

 0-7803-8966-2/05/$20.00 © 2005 IEEE